Increase in $|S_L|$ induced by channel coupling: the case of deuteron scattering

Increase in $|S_L|$ induced by channel coupling: The case of deuteron breakup

R. S. Mackintosh*
Department of Physical Sciences, The Open University, Milton Keynes, MK7 6AA, United Kingdom

D. Y. Pang†
School of Physics and Nuclear Energy Engineering, Beihang University, Beijing, 100191, China

(Received 26 July 2012; published 9 October 2012)

For deuteron scattering from ^{58}Ni at laboratory energies of 56, 79, and 120 MeV, we study the dynamic polarization potentials (DPPs) induced by S-wave and D-wave breakup (BU), separately and together, in order to gain insight into the nature of the DPP as well as a counterintuitive property: the existence of L values for which the BU coupling increases $|S_L|$, a 'wrong-way' effect. The effect is associated with the existence of emissive regions in the imaginary DPP, suggesting a connection with the nonlocal nature of the DPP. The same relationship was previously found for ^{6}Li scattering, indicating a generic effect bearing on the dynamics of nuclear reactions.

DOI: 10.1103/PhysRevC.86.047602 PACS number(s): 25.45.De, 24.50.+g, 24.10.Ht, 24.10.Eq

I. INTRODUCTION

Reference [1] presented a study of the dynamic polarization potential (DPP) due to projectile breakup for ^{6}Li nuclei scattering from ^{12}C at energies from 90 to 318 MeV. At the lower energies, and for certain values of partial-wave angular momentum L, the magnitude $|S_L|$ of the elastic channel S matrix went the 'wrong way' (WW) when coupling to the breakup channels was switched on, i.e., $|S_L|$ increased. For these values of L, channel coupling *reduced* the absorption from the elastic channel. There appeared to be an association between this occurrence and the appearance of generative (emissive) regions in the local equivalent dynamic polarization potential.

This WW phenomenon was noted long ago [2] and occurs in other scattering cases, for example, ^{6}He scattering at energies near the barrier [3–5]. In that case, too, emissive regions appear in the imaginary part of the DPP due to breakup (BU). Not all cases of channel coupling result in a WW effect. For example, the reaction channel coupling of protons to deuteron channels modifies the proton elastic $|S_{lj}|$ the 'right way.' There appears to be a correlation: with $p \leftrightarrow d$ (no WW), the change in total cross section in the elastic channel due to the coupling far exceeds the cross section to the deuteron reaction channels; however, with BU of ^{6}Li [1], the reverse is the case and the BU cross section is greater than the increase in total reaction cross section that occurs with BU coupling. In the case of $p \leftrightarrow d$ coupling, the other correlate with WW, noted above, the presence of emissive regions in the DPP, occurs only slightly in the surface region; see Ref. [6]. The WW phenomenon appears to be one effect of the nonlocality of the DPP. In line with Austern's discussion [7], the coupling removes flux from the interaction region returning (some of it) elsewhere in the nucleus.

This work is not a comprehensive study of the effect of coupled channels on deuteron scattering; that would require the inclusion of $(d \leftrightarrow p)$ and $(d \leftrightarrow t)$ couplings and many other processes. It is also not a comprehensive study of the effect of projectile breakup on deuteron scattering; that would require a more complete description of the deuteron and its breakup. It is a study, based mainly on deuteron breakup, of an anomalous generic feature of scattering that seems to be related to nonlocal effects of channel coupling.

II. CDCC CALCULATIONS

Continuum discretized coupled channels (CDCC) calculations were carried out, with the standard formalism using the code FRESCO [8], in order to study the contribution of deuteron breakup (BU) to the effective deuteron-nucleus interaction. Calculations included coupling to the S-wave continuum (SBU), the D-wave continuum (DBU), and both continua (SDBU) since we had observed different degrees of WW for the SBU and SDBU cases. The deuteron was described as an S-wave state in a Gaussian potential: $V(r) = 72.15 \times \exp[-(r/1.484)^2]$ MeV. Nuclear and Coulomb breakup were included and the maximum multipole order in the expansion of the coupling potentials was $q = 4$. The continuum discretization was specified by $k_{\max} = 1.0$ fm^{-1}, with $\Delta k = 0.05$ fm^{-1}, i.e., continuum energies up to 42 MeV.

Proton-target and neutron-target potentials were determined by renormalizing the potentials of the Bruyères Jeukenne-Lejeune-Mahaux (JLMB) folding model [9]. The measured experimental data were fitted in a grid search by the elastic scattering angular distributions for SDBU calculations. The elastic scattering angular distributions for SBU and DBU calculations will not be fitted, but the DPPs will not depend strongly upon these potentials. Fitting the angular distributions for SDBU calculations was a suitable compromise context for studying the DPPs for all cases. In the SDBU case there is full coupling between the states in the S-wave and D-wave continua.

The JLMB normalization factors for each energy presented in Table I are quite close to unity. The last two columns of this table give the volume integrals of the resulting deuteron-nucleus folded potential, the 'bare potential' for that energy. Subtracting this from the potentials found by inverting the

*r.mackintosh@open.ac.uk
†dypang@buaa.edu.cn

TABLE I. Real and imaginary renormalization factors N_R and N_I for the p-^{58}Ni and n-^{58}Ni potentials. The last two columns give volume integrals of the real and imaginary components of the folded d-^{58}Ni potential in MeV fm^3.

E_{lab}	N_R	N_I	J_R	J_I
56.0	0.90	1.05	341.25	102.18
79.0	0.95	1.05	330.33	106.30
120.0	0.95	1.05	280.88	108.49

elastic channel S-matrix from the CDCC calculations yields the DPPs presented below. The maximum radius for the CCDC calculations was 60 fm with a step size of 0.05 fm, satisfactory for elastic scattering. The Coulomb radius was $1.25 \times 58^{1/3}$ fm. No spin-orbit interactions were included. The fits to the angular distributions are presented in Fig. 1.

III. THE ANOMALOUS BEHAVIOR OF $|S_L|$ FOR DEUTERON SCATTERING

Figure 2 shows three representative cases of the effect of breakup coupling on the magnitude $|S_L|$ of the elastic channel S matrix. In Fig. 2(a) for 56 MeV and S-wave breakup, the coupling increases $|S_L|$ over two partial waves, $L = 11$ and $L = 12$. In Fig. 2(b) for 79 MeV and D-wave breakup, $|S_L|$ is slightly increased for just one L. In Fig. 2(c) for 120 MeV and both S- and D-wave breakup, there is no increase in $|S_L|$ for any L. These three cases are referred to in Table II, discussed below, as showing WW, only just showing WW, and not showing WW. For the 56 MeV cases not shown, both DBU and SDBU cases show WW for one L value rather than the two for SBU.

IV. CALCULATION OF DPP

For each energy, the bare potential is subtracted from the potential found by inverting [10,11] the elastic channel S matrix, S_L, from the CDCC calculations. The difference is the DPP (actually, the local equivalent of the formal nonlocal and L-dependent DPP) arising from the breakup coupling for that energy. The characteristics of the resulting DPPs are presented in Table II: the volume integrals, ΔJ_R and ΔJ_I, of the real and imaginary parts of the DPPs are calculated by subtracting the corresponding volume integral of the bare potential from that of the inverted potential. We also present the differences in the rms radii, ΔR_R and ΔR_I, due to breakup coupling, $\Delta\sigma_{reac}$, the change in total reaction cross section induced by breakup, and the cross section, CDCC σ_{BU}, into the particular breakup channels that were included. The SBU column presents the results for the case with S-wave breakup channels only, the DBU column is for D-wave breakup, and the SDBU column is for both S-wave and D-wave continua included and coupled together. The last column presents the numerical sums of the quantities for S-wave breakup and D-wave breakup for comparison with SDBU values. The sum has some significance for ΔJ_R and ΔJ_I, but we include the sums for ΔR_R and ΔR_I as well, and comment on the results. The line labeled 'Emissive' indicates whether there is an emissive region in the imaginary part of the DPP around 4 fm, as will be seen in figures presented below. All potentials exhibit an emissive region near the nuclear center. The last line indicates whether there are partial waves for which $|S_l|$ goes the wrong way (WW), i.e., increases, when the indicated coupling is included.

From Table II we note a link between WW and an emissive region in the DPP. The WW effect appears to be strongest at lower energies, and is *inhibited* by D-wave BU.

In the SDBU column of Table II, the line CDCC σ_{BU} presents the separate SBU and DBU cross sections to both the S-wave BU channels and D-wave BU channels and their sum, the total BU cross section. The individual values are much less than for the SBU and DBU calculations.

The following cases have a cross section to the BU channels that exceeds the increase in total cross section induced by

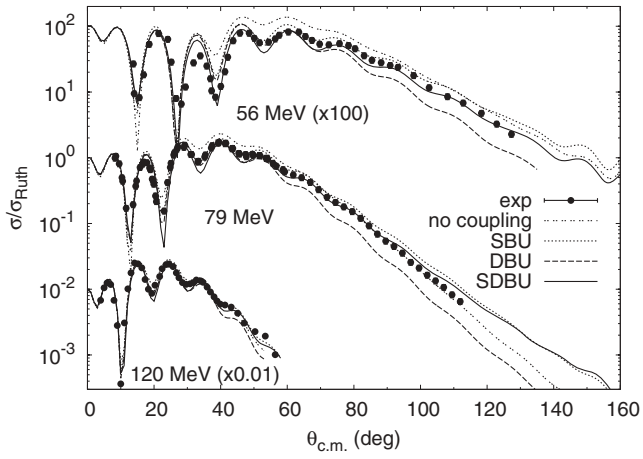

FIG. 1. For 56, 79, and 120 MeV deuterons on ^{56}Ni, the fit to the experimental angular distributions (large dots) with no coupling (double dotted line), S-wave breakup (dots), D-wave breakup (small dashes), and the full CDCC calculation with S-wave and D-wave breakup (solid line).

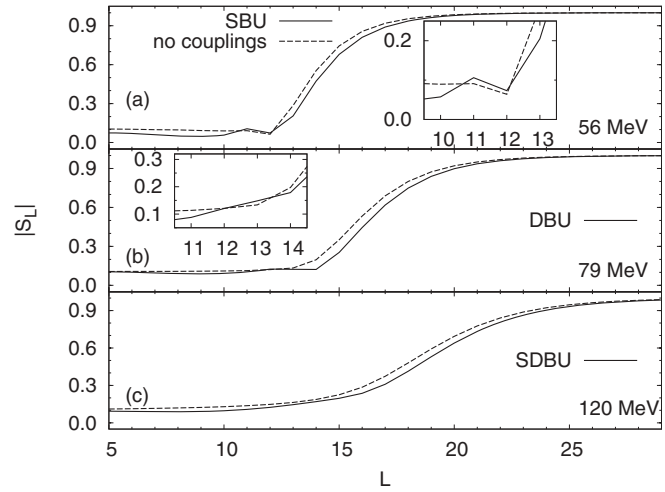

FIG. 2. For deuterons on ^{56}Ni, the magnitude of the elastic scattering matrix, $|S_L|$. The dashed lines are for no coupling to breakup channels and the solid lines are for coupling included as follows: (a) 56 MeV, S-wave breakup, (b) 79 MeV, D-wave breakup, and (c) 120 MeV, S- and D-wave breakup.

TABLE II. For deuteron scattering from ^{58}Ni, volume integrals ΔJ (in MeV fm^3) of the real and imaginary DPPs induced by projectile breakup. Convention used: Positive is attractive or absorptive.

Quantity	SBU	DBU	SDBU	SBU + DBU
		56 MeV		
ΔJ_R	4.77	−6.24	−1.55	− 1.47
ΔJ_I	15.25	15.06	18.29	30.31
ΔR_R	−0.042	−0.0628	−0.141	− 0.1048
ΔR_I	0.0643	0.2245	0.1956	0.2888
$\Delta\sigma_{reac}$	90.4	86.6	86.7	177.0
CDCC σ_{BU}	84.65	88.25	83.62 = 32.31 + 51.31	172.90
Emissive ?	yes	yes	yes	
WW ?	yes	yes	yes	
		79 MeV		
ΔJ_R	3.67	−4.65	−0.85	− 0.98
ΔJ_I	13.19	12.36	17.11	25.55
ΔR_R	−0.0406	−0.0659	−0.135	− 0.1065
ΔR_I	0.0390	0.2066	0.1649	0.2465
$\Delta\sigma_{reac}$	76.7	86.2	93.40	162.9
CDCC σ_{BU}	75.35	93.76	97.36 = 32.07 + 65.29	169.11
Emissive ?	yes	yes	yes, small	
WW ?	yes	yes, just	no	
		120 MeV		
ΔJ_R	1.90	−2.55	−0.72	− 0.65
ΔJ_I	9.59	7.66	13.57	17.25
ΔR_R	−0.0346	−0.0634	−0.1165	− 0.0980
ΔR_I	0.0080	0.1415	0.0983	0.1395
$\Delta\sigma_{reac}$	49.4	63.2	76.1	112.6
CDCC σ_{BU}	52.17	75.86	90.12 = 27.17 + 62.41	128.03
Emissive ?	yes	yes	no	
WW ?	yes, weak	no	no	

the BU coupling: DBU at 56 MeV; DBU and SDBU at 79 MeV; SBU, DBU, and SDBU at 120 MeV. This suggests the suppression of fusion by breakup, a well-known effect at lower energies.

The sums in the last column of Table II agree quite well for the real, but not imaginary, DPPs. The ΔJ_R values agree even though they are small in magnitude as a result of subtraction between substantial surface repulsion and interior attractive effects. We show below that in the asymptotic radial range (7 fm and beyond), the SBU and DBU real DPPs add quite closely to the SDBU real DPP. In Ref. [12] and references therein, the lack of additivity of DPPs for channels that are not mutually coupled provided evidence for the nonlocality of the underlying DPP, but in the present case it was not possible to switch off the coupling between the S-wave and D-wave continua. Thus it is the near additivity of J_R, not the nonadditivity of J_I, that is noteworthy. The sum of the SBU and DBU breakup cross sections greatly exceeds the SDBU breakup cross section, in line with the nonadditivity of ΔJ_I.

The radial forms of the real and imaginary parts of the DPPs are presented for 56, 79, and 120 MeV in Figs. 3–5. The DPPs behave in a very regular way, falling somewhat in magnitude with increasing energy. Concerning the real DPP, we note that for SBU it is mostly attractive, with only weak surface repulsion, whereas for DBU it is much more repulsive in the surface. The SDBU DPP shows clear surface repulsion and interior attraction. The repulsive-tending bump at all energies near 3.5 fm almost makes the DPP repulsive at 56 MeV. The total (bare plus DPP) real potential is attractive for all r but its rms radius is reduced at all energies.

The overall shape of the imaginary DPP varies regularly with energy. The absorption has a maximum magnitude in the

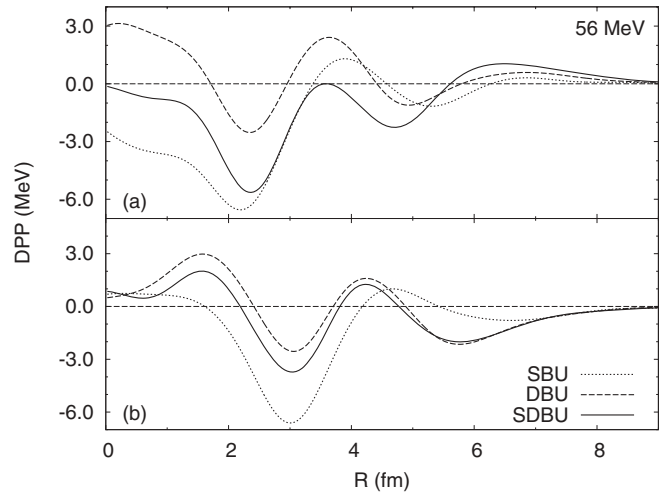

FIG. 3. For 56 MeV deuterons on ^{56}Ni, (a) the real and (b) the imaginary components of the DPP generated by S-wave breakup (dots), D-wave breakup (short dashes), and for S-wave and D-wave breakup included together (solid line).

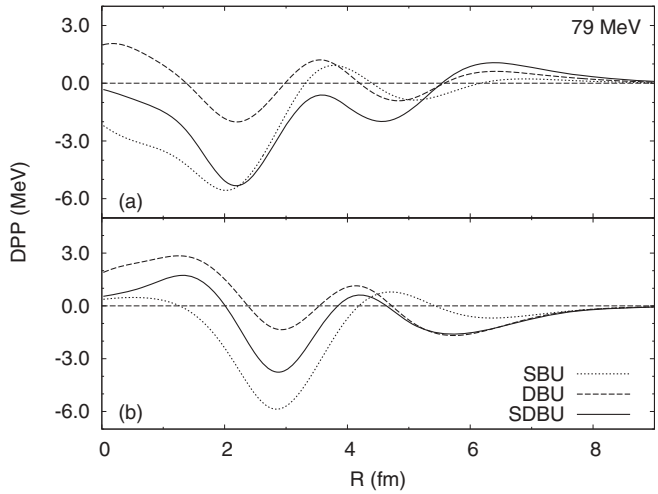

FIG. 4. For 79 MeV deuterons on ^{56}Ni, as for Fig. 3.

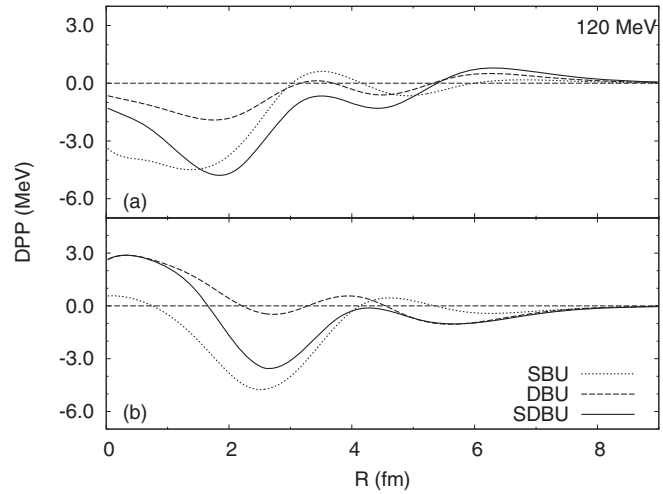

FIG. 5. For 120 MeV deuterons on ^{56}Ni, as for Fig. 3.

surface around 6 fm, which is greatest at low energies. There is an emissive peak at the nuclear center at all energies. More significant is the bump at around 4 fm that becomes emissive at 79 MeV and especially at 56 MeV. We postulate a connection between this emissiveness and the tendency for a WW effect that is most pronounced at the lowest energy. The systematic features of the DPP are consistent with the generic properties presented long ago [13].

Is the emissivity near 4 fm, apparently associated with WW, of empirical significance? In the case of ^{6}Li [1], a notch test showed that the emissive region in the DPP was within the radial range that could be sensitive to elastic scattering. Deuteron scattering is much more sensitive to the nuclear interior; see, e.g. the model-independent fitting of Ermer *et al*. [14]. Their model-independent potential for 52 MeV deuterons scattering from ^{40}Ca revealed emissive regions in the full potential, not just DPPs. The present work makes that more plausible. It might be interesting to modify the central potential to remove the emissive feature near $r = 0$, examine its effect on the angular distribution, and verify that it is not associated with the WW effect.

V. GENERIC EFFECT: COMPARISON WITH ^{6}Li ON ^{12}C

The above calculations were prompted by the results of Ref. [1] where a relationship between WW effects and emissive regions appeared in the DPP due to breakup of ^{6}Li on ^{12}C. Figure 9 of that paper shows the trend of how $|S_L|$ is modified by BU of ^{6}Li for five energies from 90 to 380 MeV. We restate here the key facts: At 90 MeV, WW occurs for $L = 12$ (slightly), $L = 13$ ($|S_L|$ almost doubled), and $L = 14$ ($|S_L|$ increased by about 70%) and the imaginary DPP becomes emissive by almost 3 MeV between 2 and 3 fm. At 123.5 MeV, $|S_L|$ has a bump at $L = 11$ but just misses going WW, while the DPP has an emissive peak with a maximum value of about 2 MeV. At 168.6 MeV there is neither WW nor an emissive region. Finally, we note that the extent to which the BU cross section exceeds the increase in reaction cross section due to breakup falls with energy, the ratio being 2.91 at 90 MeV, 2.35 at 123.5 MeV, and 2.18 at 168.6 MeV. There appears to be a generic effect of projectile breakup.

We intend to carry out ψ-potential studies [15,16] of these and similar cases to investigate the spatial distribution of absorption and emission within the target nucleus. This might throw light on the causation of WW and its relationship to Austern's account [7] of nonlocality in nuclear interactions, a fundamental aspect nuclear interaction dynamics. We note a contemporary requirement [17] for a precise understanding of deuteron reactions.

ACKNOWLEDGMENT

This work is supported by the the National Natural Science Foundation of China (Nos. 11035001 and 11275018).

[1] D. Y. Pang and R. S. Mackintosh, Phys. Rev. C **84**, 064611 (2011).
[2] R. S. Mackintosh and A. A. Ioannides, in *Advanced Methods in the Evaluation of Nuclear Scattering Data, Lecture Notes in Physics 236* (Springer-Verlag, Berlin, 1985), p. 283.
[3] R. S. Mackintosh and N. Keeley, Phys. Rev. C **70**, 024604 (2004).
[4] R. S. Mackintosh and N. Keeley, Phys. Rev. C **79**, 014611 (2009).
[5] N. Keeley, R. S. Mackintosh, and C. Beck, Nucl. Phys. A **834**, 792c (2010).
[6] R. S. Mackintosh and N. Keeley, Phys. Rev. C **85**, 064603 (2012).
[7] N. Austern, Phys. Rev. B **137**, 752 (1965).
[8] I. J. Thompson, Comput. Phys. Rep. **7**, 167 (1988).
[9] E. Bauge, J. P. Delaroche, and M. Girod, Phys. Rev. C **63**, 024607 (2001).

[10] V. I. Kukulin and R. S. Mackintosh, J. Phys. G: Nucl. Part. Phys **30**, R1 (2004).
[11] R. S. Mackintosh, arXiv:1205.0468 (2012).
[12] R. S. Mackintosh and N. Keeley, Phys. Rev. C **81**, 034612 (2010).
[13] A. A. Ioannides and R. S. Mackintosh, Phys. Lett. B **161**, 43 (1985).
[14] M. Ermer, H. Clement, P. Grabmayr, G. J. Wagner, L. Friedrich, and E. Huttel, Phys. Lett. B **188**, 17 (1987).
[15] R. S. Mackintosh, A. A. Ioannides, and S. G. Cooper, Nucl. Phys. A **483**, 173 (1988).
[16] S. G. Cooper and R. S. Mackintosh, Nucl. Phys. A **511**, 29 (1990).
[17] S. J. Freeman and J. P. Schiffer, arXiv:1207.4290.